Autonomous Calibration of Single-Loop Closed Kinematic Chains Formed by Manipulators with Passive Endpoint Constraints

David J. Bennett, *Student Member, IEEE,* and John M. Hollerbach, *Member, IEEE*

Abstract—**A serial-link manipulator may form a mobile closed kinematic chain when interacting with the environment, if it is redundant with respect to the task degrees of freedom (DOF's) at the endpoint. If the mobile closed chain assumes a number of configurations, then loop consistency equations permit the manipulator and task kinematics to be calibrated simultaneously using only the joint angle readings; endpoint sensing is not required. Example tasks include a fixed endpoint (0-DOF task), the opening of a door (1-DOF task), and point contact (3-DOF task). Identifiability conditions are derived for these various tasks.**

I. Introduction

KINEMATIC calibration is important for model-based robot control [1]. We [15] and many other authors (see reviews in [14], [17]) have developed open-loop methods that estimate the geometric and static nongeometric kinematic parameters of open-chain manipulators by relying on special purpose pre-calibrated endpoint locating systems, such as precision points or camera-based measurement systems. Section II summarizes our open-loop method, which is the starting point for our new method; new results on the identifiability of the open-loop method are also provided.

Our new method, which we call *closed-loop kinematic calibration,* eliminates the need for endpoint locating systems: *if a manipulator is formed into a mobile closed kinematic chain, then its joint angle readings alone are enough to identify the kinematic parameters.* A manipulator may form a mobile closed-loop kinematic chain if it is redundant with respect to its endpoint constraint (task). Section III considers the simplest endpoint constraint: the position and orientation of the endpoint are fixed relative to the base link. For this 0-DOF task, the manipulator must be redundant (≥ 7 DOF's) to form a mobile closed loop. For each loop configuration there are three position and three orientation loop consistency equations. If the closed loop is placed into n configurations (with the same endpoint location), there result $6n$ equations that may be solved for the unknown parameters.

An equivalent scenario is two manipulators rigidly attached together at their endpoints with a combined total of DOF's ≥ 7 (Fig. 1). The last link of the second manipulator may be defined as the base, and the entire closed kinematic chain may be viewed as a single equivalent manipulator.

Section IV then considers two endpoint constraints with passive degrees of freedom: 1) rotation about a passive revolute joint (e.g., opening a door), and 2) rotation about a passive spherical joint (e.g., point contact). For constraint 1, a nonredundant 6-DOF manipulator can form a *mobile* closed loop, whereas for constraint 2 a 4-DOF manipulator could suffice. In general, for each passive degree of freedom introduced into the endpoint constraint one less degree of freedom is required by the manipulator. As a corollary, the geometry of the task can also be identified, for example, the position and orientation of the revolute joint in constraint 1.

Several technicalities were overcome in developing this closed-loop method. A theorem was developed to determine which parameters are identifiable in the consistency equations. We also show how the passive DOF's can be eliminated from the endpoint constraint for the two cases studied and mention how to do this in general. Third, we apply a Newton-like search method for the kinematic parameters, which starts from an initial guess at the parameters. Simulations will demonstrate the convergence of the method. Finally, the manipulator must be able to make constrained internal joint movements, without knowing the true kinematic parameters or producing excessive internal or endpoint forces.

Closed-loop kinematic calibration is related to mechanism synthesis [11], which characterizes closed-loop mechanisms with one degree of mobility through relative displacements of designated input and output angles. By eliminating (with difficulty) the five unspecified DOF's from the kinematic

Manuscript received February 23, 1989; revised March 27, 1990. This work was supported in part by the University Research Initiatives under Office of Naval Research Contract N00014-86-K-0180 and in part by the Advanced Research Projects Agency of the Department of Defense under Office of Naval Research Contract N00014-85-K-0124. J. M. Hollerbach was also supported by an NSF Presidential Young Investigator Award. D. J. Bennett was also supported by a Fairchild Fellowship and a scholarship from the Natural Sciences and Engineering Research Council of Canada. Portions of this paper were presented at the IEEE Conference on Robotics and Automation, Scottsdale, AZ, May 1989.

D. J. Bennett is with the Artificial Intelligence Laboratory, Massachusetts Institute of Technology, Cambridge, MA 02139.

J. M. Hollerbach was with the Artificial Intelligence Laboratory, Massachusetts Institute of Technology, Cambridge, MA 02139. He is now with the Departments of Mechanical Engineering and Biomedical Engineering, McGill University, Montreal, Quebec, Canada H3A 2B4.

IEEE Log Number 9102375.

1042-296X/91$01.00 ©1991 IEEE

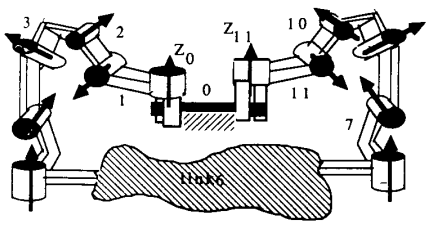

Fig. 1. A single closed-loop kinematic chain formed by a redundant mainpulator or by dual manipulators.

equations, a displacement equation results that is a 16th-order polynomial in the tangent half-angles of the input and output angles [16]. A difference from mechanism synthesis is that serial-chain manipulators typically have sensors on all the joints and so eliminating the unsensed passive DOF's at the endpoint from the kinematic equations is considerably easier. Portions of this work have been previously reported [3]–[5].

II. Open-Loop Kinematic Calibration

This section presents our method for open-loop kinematic calibration [15], which serves to set the basic concepts and mathematics from which the closed-loop method is derived. New results in identifiability are presented for our open-loop method; these results apply more generally to similar methods that have appeared in the literature [14].

A. The Kinematic Model

Both geometric and nongeometric parameters are required for kinematic calibration. The Denavit–Hartenberg (D–H) convention [9] is employed for the geometric parameters (Fig. 2). For a manipulator with n DOF's, the end effector is located by the position vector $\mathbf{p}_c^i$ and the orientation matrix $\mathbf{R}_c^i$:

$$\mathbf{p}_c^i = \sum_{j=1}^{n} s_j \mathbf{z}_{j-1} + a_j \mathbf{x}_j \tag{1}$$

$$\mathbf{R}_c^i = \prod_{j=1}^{n} \mathbf{R}_z(\theta_j^i)\mathbf{R}_x(\alpha_j^i) \tag{2}$$

where $\mathbf{R}_z(\phi)$ and $\mathbf{R}_x(\phi)$ are 3×3 rotation matrices about the $\mathbf{z}$ and $\mathbf{x}$ axes by the angle ϕ, and the subscript c indicates that the position and orientation are computed from the model. The superscript i refers to the configuration of the manipulator, since in kinematic calibration it is placed into a number of configurations $\underline{\theta} = (\theta_1^i, \ldots, \theta_m^i)$, $i = 1, \cdots, m$. The required geometric parameters are s_j, α_j, and a_j for links $j = 1, \ldots, n$.

The nongeometric parameters are focused at a joint and reflect errors between the true and measured joint angle; sources of error include backlash, gear eccentricity, joint compliance, and joint angle offset. We model only the joint angle offset error θ_j^{off}, which needs to be identified. It is related to the actual θ_j' and measured θ_j D–H joint angles by $\theta_j' = \theta_j + \theta_j^{\text{off}}$. All of the unknown kinematic parameters are placed into a single vector $\underline{\varphi} = (\underline{\theta}^{\text{off}}, \underline{\alpha}, \underline{s}, \underline{a})$, where $\underline{s} = (s_1, \ldots, s_n)$, etc.

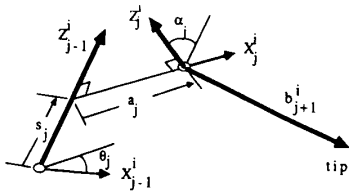

Fig. 2. Denavit–Hartenberg coordinates and tip vector $\mathbf{b}_j^i$.

Instead of the orientation matrix $\mathbf{R}_c^i$, it is convenient to represent the orientation by the vector $\underline{\rho}_c^i = (\phi_x^i, \phi_y^i, \phi_z^i)$, representing the roll-pitch-yaw (ZYX) Euler angles: $\mathbf{R}_c^i = \mathbf{R}_z(\phi_z^i)\mathbf{R}_y(\phi_y^i)\mathbf{R}_x(\phi_x^i)$. The computed endpoint location $\underline{x}_c^i = (\underline{\rho}_c^i, \mathbf{p}_c^i)$ may then be written as

$$\underline{x}_c^i = \underline{f}\left(\underline{\theta}^i, \underline{\varphi}\right) \tag{3}$$

where the function f is derived from (1) and (2). Its exact form is not required here.

B. Iterative Identification

To estimate $\underline{\varphi}$, the manipulator must be moved into an adequate number m of configurations, in consideration of the large number of parameters in $\underline{\varphi}$ and of statistical averaging. At each configuration i the actual endpoint location $\underline{x}_a^i$ is measured. The goal is to determine the $\underline{\varphi}$ that best predict from the kinematic model (3) all of the endpoint measurements $\mathcal{X} = (\underline{x}_a^1, \ldots, \underline{x}_a^m)$:

$$\mathcal{X} = \mathcal{F}(\underline{\varphi}) \tag{4}$$

where $\mathcal{F}(\underline{\varphi}) = (f(\underline{\theta}^1, \underline{\varphi}), \ldots, f(\underline{\theta}^m, \underline{\varphi}))$.

Solving for $\underline{\varphi}$ from (4) is a nonlinear estimation problem, which can be done by linearization and iteration:

$$\Delta\mathcal{X} = \mathcal{C}\Delta\underline{\varphi} \tag{5}$$

where $\mathcal{C} = \partial\mathcal{F}/\partial\underline{\varphi}$. We can consider $\Delta\mathcal{X} = (\Delta\underline{x}^1, \ldots, \Delta\underline{x}^m)$, with $\Delta\underline{x}^i = \underline{x}_a^i - \underline{x}_c^i$, as the location errors. Similarly, $\Delta\underline{\varphi} = \underline{\varphi} - \underline{\varphi}_0$ is the error in the total parameter set, where $\underline{\varphi}_0$ is the current estimate and $\underline{\varphi}$ is the corrected estimate. In $\Delta\underline{\varphi}$, $\Delta\underline{s} = \underline{s} - \underline{s}_0$, etc. An estimate of the parameter errors is provided by minimizing $LS = (\Delta\mathcal{X} - \mathcal{C}\Delta\underline{\varphi})^T(\Delta\mathcal{X} - \mathcal{C}\Delta\underline{\varphi})$, which yields

$$\Delta\underline{\varphi} = \left(\mathcal{C}^T\mathcal{C}\right)^{-1}\mathcal{C}^T\Delta\mathcal{X}. \tag{6}$$

Finally, the guess at the parameters is updated as $\underline{\varphi} = \underline{\varphi}_0 + \Delta\underline{\varphi}$ and the iteration continues until $\Delta\mathcal{X} \to 0$.

The basis for linearization is the assumption that $\underline{x}_c^i$ is close to $\underline{x}_a^i$. Then

$$\Delta\underline{x}^i = \underline{x}_a^i - \underline{x}_c^i = \begin{bmatrix} \Delta\underline{\rho}^i \\ \Delta\mathbf{p}^i \end{bmatrix} \tag{7}$$

where $\Delta\underline{\rho}^i = (\partial\phi_x^i, \partial\phi_y^i, \partial\phi_z^i)$ is the incremental orientation error in terms of the Euler angles and $\Delta\mathbf{p}^i = (dx^i, dy^i, dz^i)$ is the incremental position error. When $\underline{\varphi}_0$ is far from the final values, problems with this approach may occur, as discussed later.

The differential of (3) is

$$\Delta \underline{x}^i = \frac{\partial \underline{x}_c^i}{\partial \underline{\theta}} \Delta \underline{\theta} + \frac{\partial \underline{x}_c^i}{\partial \underline{\alpha}} \Delta \underline{\alpha} + \frac{\partial \underline{x}_c^i}{\partial \underline{s}} \Delta \underline{s} + \frac{\partial \underline{x}_c^i}{\partial \underline{a}} \Delta \underline{a} = \mathbf{C}^i \Delta \underline{\varphi} \quad (8)$$

where

$$\mathbf{C}^i = \frac{\partial \underline{x}_c^i}{\partial \underline{\varphi}} = \left[\frac{\partial \underline{x}_c^i}{\partial \underline{\theta}} \frac{\partial \underline{x}_c^i}{\partial \underline{\alpha}} \frac{\partial \underline{x}_c^i}{\partial \underline{s}} \frac{\partial \underline{x}_c^i}{\partial \underline{a}} \right]$$

and $\mathscr{C} = (\mathbf{C}^1, \ldots, \mathbf{C}^m)$. The Jacobian $\mathbf{C}^i$ is often formed through the use of differential homogeneous transformations, but to address identifiability we find the use of screw coordinates more convenient and transparent [20], [24], [26]. To proceed, we must express differential rotations $\Delta \mathbf{r}^i = (\partial x^i, \partial y^i, \partial z^i)$ about orthogonal axes rather than the differential rotations $\Delta \underline{\rho}^i$ about nonorthogonal axes. The two may be related by a matrix $\mathbf{Q}^i$, whose form depends on the particular Euler angles (ZYX here) chosen ([25]):

$$\Delta \mathbf{r}^i = \begin{bmatrix} 1 & 0 & -\sin \phi_y^i \\ 0 & \cos \phi_z^i & \sin \phi_z^i \cos \phi_y^i \\ 0 & -\sin \phi_z^i & \cos \phi_z^i \cos \phi_y^i \end{bmatrix} \Delta \underline{\rho}^i = \mathbf{Q}^i \Delta \underline{\rho}^i. \quad (9)$$

Assuming the inverse of $\mathbf{Q}^i$ exists, then

$$\Delta \underline{x}^i = \begin{bmatrix} \Delta \underline{\rho}^i \\ \Delta \mathbf{p}^i \end{bmatrix} = \begin{bmatrix} (\mathbf{Q}^i)^{-1} & \mathbf{0} \\ \mathbf{0} & \mathbf{I} \end{bmatrix} \begin{bmatrix} \Delta \mathbf{r}^i \\ \Delta \mathbf{p}^i \end{bmatrix} = \underline{\Omega}^i \begin{bmatrix} \Delta \mathbf{r}^i \\ \Delta \mathbf{p}^i \end{bmatrix} \quad (10)$$

where a 6×6 matrix $\underline{\Omega}^i$ has been defined incorporating 3×3 zero matrices $\mathbf{0}$ and identity matrix $\mathbf{I}$.

The matrix $\mathbf{Q}^i$ is not invertible when $\phi_y^i = \pi/2$, which is the singularity for this set of Euler angles. This problem is inescapably linked with the use of Euler angles, since no set of Euler angles exists that is the integral of angular velocity. At endpoint configurations with $\phi_y^i = \pi/2$ an alternate Euler angle formulation (say ZXZ) may be used to guarantee that $\mathbf{Q}^i$ is always invertable. Without loss of generality we assume that appropriate Euler representations will be used for these few singular endpoint configurations and do not discuss them further.

The total incremental displacement $(\Delta \mathbf{r}^i, \Delta \mathbf{p}^i)$ is the sum of the instantaneous screws corresponding to variations in all of the parameters:

$$\begin{bmatrix} \Delta \mathbf{r}^i \\ \Delta \mathbf{p}^i \end{bmatrix} = \sum_{j=1}^{n} \Delta \theta_j \begin{bmatrix} \mathbf{z}_{j-1}^i \\ \mathbf{z}_{j-1}^i \times \mathbf{b}_j^i \end{bmatrix} + \Delta \alpha_j \begin{bmatrix} \mathbf{x}_j^i \\ \mathbf{x}_j^i \times \mathbf{b}_{j+1}^i \end{bmatrix} + \Delta s_j \begin{bmatrix} \mathbf{0} \\ \mathbf{z}_{j-1}^i \end{bmatrix} + \Delta a_j \begin{bmatrix} \mathbf{0} \\ \mathbf{x}_j^i \end{bmatrix} \quad (11)$$

where $\mathbf{b}_{j+1}^i$ is a vector from the jth coordinate system to the endpoint (Fig. 2). From the parameter-based screws on the right, Jacobian matrices can be formed whose columns j are

$$(\mathbf{J}_\theta^i)_j = \begin{bmatrix} \mathbf{z}_{j-1}^i \\ \mathbf{z}_{j-1}^i \times \mathbf{b}_j^i \end{bmatrix}, \quad (\mathbf{J}_\alpha^i)_j = \begin{bmatrix} \mathbf{x}_j^i \\ \mathbf{x}_j^i \times \mathbf{b}_{j+1}^i \end{bmatrix},$$

$$(\mathbf{J}_s^i)_j = \begin{bmatrix} \mathbf{0} \\ \mathbf{z}_{j-1}^i \end{bmatrix}, \quad (\mathbf{J}_a^i)_j = \begin{bmatrix} \mathbf{0} \\ \mathbf{x}_j^i \end{bmatrix} \quad (12)$$

where $\mathbf{J}_\beta^i$ represents a Jacobian with regard to a particular parameter vector β; thus $\mathbf{J}_\theta^i$ is the ordinary Jacobian related to joint angle displacement. More compactly,

$$\begin{bmatrix} \Delta \mathbf{r}^i \\ \Delta \mathbf{p}^i \end{bmatrix} = [\mathbf{J}_\theta^i \, \mathbf{J}_\alpha^i \, \mathbf{J}_s^i \, \mathbf{J}_a^i] \Delta \underline{\varphi} = \mathbf{A}^i \Delta \underline{\varphi}. \quad (13)$$

From (13) and (10), the ensemble Jacobian $\mathbf{A}^i$ is then related to the Jacobian $\mathbf{C}^i$ by $\mathbf{C}^i = \underline{\Omega}^i \mathbf{A}^i$. Define $\mathscr{A} = (\mathbf{A}^1, \ldots, \mathbf{A}^m)$.

C. Identifiability

Next we derive several results pertaining to the identifiability of $\underline{\varphi}$ in (4). First we establish that the solution cannot be globally unique.

Theorem 1: There are at least 2^{n-1} solutions $\underline{\varphi}$ to (4).

Proof: We presume that at least one solution $\underline{\varphi}$ exists because the data come from a physical system. Additional solutions may be derived from this $\underline{\varphi}$. There are two possible parameter sets per joint. For a fixed $\mathbf{z}_j^i$, the $\mathbf{x}_j^i$ axis can be made to point in opposite directions by adding 180° onto θ_j^{off}; to accommodate this change, the sign is changed on a_j and α_j while s_j is unchanged. At the endpoint, the directions $\mathbf{x}_n^i$ and $\mathbf{z}_n^i$ are specified by the position requirement. Hence, we have generated 2^{n-1} solutions from the original solution $\underline{\varphi}$. ■

Although there are multiple solutions, in practice kinematic calibration starts off with a rough estimate $\underline{\varphi}_0$ and searches locally for a solution. Thus, the relevant question is whether or not there is a unique solution within a small region of the parameter space. We draw on some results from differential topology [10], [22].

Definition 1 (Locally Unique): A solution $\underline{\varphi}'$ to (4) is locally unique if it is the only solution in an arbitrarily small neighborhood (ball) around $\underline{\varphi}'$.

In addition to uniqueness, we also want to know if a well-behaved inverse function $\mathscr{F}^{-1}$ exists to generate the solution $\underline{\varphi}'$.

Definition 2 (Locally Identifiable): A smooth function $\mathscr{X} = \mathscr{F}(\underline{\varphi})$ is locally identifiable at $\underline{\varphi}'$ if (1) $\underline{\varphi}'$ is locally unique, and (2) there exists a smooth inverse function $\mathscr{F}^{-1}$ such that $\mathscr{F}^{-1}(\mathscr{F}(\underline{\varphi})) = \underline{\varphi}$.

A smooth function has continuous partial derivatives of all orders. Notice that the existence of a smooth inverse function in part 2 of the definition does not guarantee uniqueness (part 1).

If the number of equations equals the number of unknown parameters, then local identifiability is equivalent to requiring that $\mathscr{F}$ is a *local diffeomorphism*. It is established in [10] that $\mathscr{F}$ is a local diffeomorphism if and only if the square Jacobian matrix $\mathscr{C} = [\partial \mathscr{F} / \partial \underline{\varphi}']$ is nonsingular. This motivates the following results for when $\mathscr{C}$ is not necessarily square. Lemma 1 is a general result that applies to all

equations of the form (4). Lemmas 2 and 3 are particular to the kinematic calibration problem.

Lemma 1: Let $\underline{\varphi}'$ be a solution to (4). The Jacobian $\mathscr{C}$ has full rank if and only if the parameters $\underline{\varphi}'$ are locally identifiable.

Proof: Assume that $\mathscr{C}$ has full rank. Let $\underline{\varphi}$ be another solution to (4). A Taylor series expansion relates $\underline{\varphi}$ to $\underline{\varphi}'$:

$$\mathscr{F}(\underline{\varphi}) = \mathscr{F}(\underline{\varphi}') + \mathscr{C}(\underline{\varphi} - \underline{\varphi}') + \cdots \tag{14}$$

where $\mathscr{F}(\varphi) = \mathscr{F}(\varphi')$. If φ is in a sufficiently small neighborhood of φ', then the higher order terms after the first differential may be neglected. Then $\mathscr{C}(\underline{\varphi} - \underline{\varphi}') = 0$. Since $\mathscr{C}$ does not have a null space, then $\underline{\varphi} = \underline{\varphi}'$, and φ' is locally unique. Furthermore, there exists a smooth inverse function $\mathscr{F}^{-1}$, as (6) suffices.

Conversely, assume that the parameters $\underline{\varphi}'$ are locally identifiable. Let $\mathscr{F}^{-1}$ be a smooth inverse function. Differentiating $\mathscr{F}^{-1}(\mathscr{F}(\varphi)) = \varphi$ by φ yields $[\partial \mathscr{F}^{-1}/\partial \mathscr{X}]$ $[\partial \mathscr{F}/\partial \varphi] = I$. If $\mathscr{C}$ does not have full rank, then there exists a vector element $\underline{n}$ of its null space. Postmultiplying by $\underline{n}$ yields $\underline{0} = \underline{n}$, a contradiction. Hence, $\mathscr{C}$ has full rank. ■

If Jacobian $\mathscr{C}$ has dependent columns, the solution to (4) is not necessarily locally unique because the higher order terms of the Taylor series expansion of $\mathscr{F}$ may be nonzero when evaluated at an element of the null space of $\mathscr{C}$. The next three lemmas require the definition of $\mathscr{C}$ by (8). The first of these lemmas allows us to cast the identifiability results in terms of the Jacobian $\mathscr{A}$.

Lemma 2: Assume that $\underline{\Omega}^i$ is invertible. Then $\mathscr{C}$ has full rank if and only if $\mathscr{A}$ does.

The proof follows straightforwardly from the definitions of $\mathscr{A}$ and $\mathscr{C}$, and the relation $\mathbf{C}^i = \Omega^i \mathbf{A}^i$ derived from (13). The following two lemmas are for the open-loop case, and do not hold for the closed-loop case in Section III.

Lemma 3: The Jacobian $\mathscr{A}$ does not have full rank if and only if there exists a constant linear relation among the $\mathbf{x}_j^i$ and $\mathbf{z}_j^i$ axes, that is,

$$\mathbf{0} = \sum_{j=1}^{n} c_j \mathbf{z}_{j-1}^i + k_j \mathbf{x}_j^i \tag{15}$$

for some constants c_j and k_j, not all zero, for all configurations $i = 1, \ldots, m$.

Proof: Part 1: Assume that $\mathscr{A}$ does not have full rank. Then there is a constant linear relation among the screw coordinates (12). Two cases must be considered. First, if this linear relation only includes the last two screw coordinates in (12), then the same linear relation must hold in the positional component of the screws, the last three rows that contain just the $\mathbf{x}_j^i$ and $\mathbf{z}_j^i$ axes. Thus (15) holds for some constants c_j and k_j, not all zero, for all configurations $i = 1, \ldots, m$. Second, if this linear relation includes the first two screws in (12), then this linear relation must hold in the rotational component of the screws, the first three rows that also contain just the $\mathbf{x}_j^i$ and $\mathbf{z}_j^i$ axes. Again, (15) holds.

Part 2: Conversely, assume that (15) holds. Then at least the screw coordinates $(\mathbf{J}_a^i)_j$ and $(\mathbf{J}_s^i)_j$ have a constant linear dependence, and $\mathscr{A}$ does not have full rank. ■

Lemma 4: $\mathscr{C}$ has full rank if and only if $\underline{\varphi}'$ is locally unique.

Proof: Assume that $\mathscr{C}$ has full rank. By Lemma 1, $\underline{\varphi}'$ is locally identifiable and hence is locally unique. Next assume φ' is locally unique. Suppose $\mathscr{C}$ does not have full rank; by Lemma 2 neither does $\mathscr{A}$. From Lemma 3 we can add (15) to (1) to change the length parameters without affecting $\mathbf{p}_c^i$. The kinematic length parameters would not be unique, contradicting the assumption. Hence $\mathscr{C}$ has full rank. ■

Theorem 2 (Identifiability): The parameters φ are locally unidentifiable or locally nonunique if and only if there exist constants c_j and k_j, not all zero, such that

$$\mathbf{0} = \sum_{j=1}^{n} c_j \mathbf{z}_{j-1}^i + k_j \mathbf{x}_j^i \tag{16}$$

for all configurations $i = 1, \ldots, m$.

Proof: This theorem follows from Lemmas 1–4.

Various categories of singularities (occurrences of (16)), which are generic to the closed-loop case as well (see Section III), will now be enumerated. These categories are meant to be illustrative rather than exhaustive. Although not expressly discussed in each category, the real problem is associated with near singular situations, which cause intractable numerical sensitivity problems while solving for the parameters.

Singularity 1: Coordinate Description: In the D–H convention, when there are two consecutive parallel joint axes, there is no unique common normal (Fig. 2). Parallel axes imply

$$\mathbf{z}_j^i - \mathbf{z}_{j-1}^i = 0. \tag{17}$$

Thus, (16) is true and the corresponding s_j and s_{j+1} may not be identified alone (although the sum $s_j + s_{j+1}$ can be identified). This situation can be avoided by changing the coordinate description of the parallel axes to a convention such as Hayati's [12], which however may not be used exclusively because it too suffers from a parameter ambiguity when two consecutive joint axes are perpendicular.

A revolute joint axis is a *line vector,* which is located by four parameters. Hence any coordinate description with greater than four parameters per link is singular (unless extra constraints are imposed). Similarly, a prismatic (linear) joint axis is a *free vector* defined by only two orientation parameters, and coordinate descriptions with more than two parameters are singular.

Singularity 2: Insufficient Excitation: If the mechanism is not moved into a sufficient number of configurations, then the data are not *sufficiently exciting* [2]. A small variation in each parameter of φ should cause an observable displacement in the end effector. The optimal data set would maximize the observable model error over variations in all of the parameters [21]. An impoverished data set would not be able to distinguish changes in particular parameters, which could vary arbitrarily. A trivial example is an immobile joint whose axes $\mathbf{x}_j^i$, $\mathbf{z}_j^i$, $\mathbf{x}_{j-1}^i$, and $\mathbf{z}_{j-1}^i$ are always linearly dependent.

Singularity 3: Transient Singularities: During the course of the iterative search, an intermediate singular parameter set may be found even though the real mechanism may not have singularities. Simulations show that this situation is surpris-

ingly common when the initial guess $\underline{\varphi}_0$ is not close to the true solution. Since this singularity is associated with the algorithm, it may be avoided by the modified minimization criteria $LS' = LS + \lambda\Delta\underline{\varphi}^T\Delta\underline{\varphi}$. In addition to minimizing the end effector tracking error, LS' minimizes the variation in parameters so that at a potential singularity the arbitrary parameters tend to remain fixed. Minimizing LS' yields

$$\Delta\underline{\varphi} = \left(\mathscr{C}^T\mathscr{C} + \lambda I\right)^{-1}\mathscr{C}^T\Delta\mathscr{X}. \tag{18}$$

Iteratively applying (18) results in the Levenberg–Marquardt algorithm [18], [19]. The free parameter λ determines the trade-off between a straight Newton iteration and a much slower gradient descent.

III. Closed-Loop Chains with Fixed Endpoints

We consider next a redundant manipulator (≥ 7 DOF's) rigidly attached to the ground at its endpoint. In general, the resulting closed-loop kinematic chain is mobile, since the fixed endpoint constrains only 6 of the DOF's of the manipulator. Our closed-loop method uses this mobility to calibrate kinematically the manipulator without endpoint sensing. The following observation is the key: the origin of coordinates can be placed at the fixed endpoint location and can be defined to have zero orientation and position. Hence, $\underline{x}_a^i = \underline{0}$, and no measurements are required because the actual endpoint location is known and is zero (by definition).

Fig. 3 illustrates this origin placement for a 7-DOF manipulator. The combined manipulator tool and ground may be viewed as a single effective link that connects the last to first joint of the manipulator. The end effector axes $\mathbf{z}_7^i$ and $\mathbf{x}_7^i$ are made coincident with the base coordinate axes $\mathbf{z}_0^i$ and $\mathbf{x}_0^i$. Note that the kinematic parameters of the ground link must now be identified.

The mathematical development in the previous section then applies, with one modification. As before, the mobile closed chain is moved into a number of configurations. At each configuration i the endpoint error follows simply from (7):

$$\Delta\underline{x}^i = -\underline{x}_c^i = -\left(\partial x_c^i, \partial y_c^i, \partial z_c^i, dx_c^i, dy_c^i, dz_c^i\right) \tag{19}$$

where $\Delta\mathbf{r}^i = (\partial x_c^i, \partial y_c^i, \partial z_c^i)$ is the computed orientation and $\Delta\mathbf{p}^i = (dx_c^i, dy_c^i, dz_c^i)$ is the computed position. Because the "measured" Euler angles are defined as zero, for the closed-loop case $\Delta\mathbf{r}^i = \Delta\underline{\rho}^i$ and $\mathbf{C}^i = \mathbf{A}^i$.

The iterative estimation procedure cannot be applied further without modification because the Jacobian $\mathscr{C}$ is singular. The position equations for the closed loop are

$$\mathbf{p}_c^i = \sum_{j=1}^{n} s_j\mathbf{z}_{j-1}^i + a_j\mathbf{x}_j^i = \mathbf{0}. \tag{20}$$

Hence, the length parameters are linearly dependent and (15) is satisfied. Intuitively, the size of the manipulator can be scaled arbitrarily and still satisfy the loop closure equations. To proceed with our closed-loop method, it is necessary to specify one length parameter to scale the size of the mechanism. For example, suppose we set $a_1 = -1$. We redefine $\underline{a} = (a_2, \ldots, a_n)$ and remove the first column from the

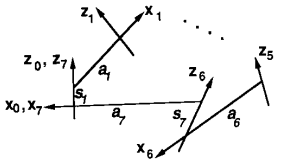

Fig. 3. Ground link definition.

Jacobian $\mathbf{J}_a^i$, which redefines $\mathbf{A}^i$ in (13). We may then proceed as before with the parameter identification. Similarly, if another parameter such as s_3 had been specified instead, analogous changes in the definition of $\underline{s}$ and $\mathbf{A}^i$ would be required. In the remainder of this paper, we vary which parameter sets the scale for convenience.

A. Identifiability

For the purposes of identifiability, we will proceed with the scaling $a_1 = -1$. The following identifiability results are couched in terms of the choice of a_1, but a different choice would result in trivial changes to the results. Of course, it is necessary in the actual mechanism that $a_1 \neq 0$. We do not consider mechanisms that have all length parameters zero (i.e., spherical mechanisms).

Theorem 1 and Lemma 1 apply intact to the closed-loop case, but Lemmas 3–4 and Theorem 2 require a slight modification. Redefine the endpoint position as

$$\mathbf{p}_c^i = \mathbf{x}_1^i = \sum_{j=1}^{n} s_j\mathbf{z}_{j-1}^i + \sum_{j=2}^{n} a_j\mathbf{x}_j^i. \tag{21}$$

Also, we must make the following definition to treat a possible exception arising from $\mathbf{x}_1^i$ being in the expression for $(\mathbf{J}_\alpha^i)_1$.

Definition 3 (Type-E Special Mechanism): A single-loop closed kinematic chain is type-e if its screw coordinates satisfy the following exceptional relation:

$$\mathbf{0} = \sum_{j=1}^{n} s_j\begin{bmatrix}\mathbf{z}_{j-1}^i \\ \mathbf{z}_{j-1}^i \times \mathbf{b}_j^i\end{bmatrix} + a_j\begin{bmatrix}\mathbf{x}_j^i \\ \mathbf{x}_j^i \times \mathbf{b}_{j+1}^i\end{bmatrix} + q_j\begin{bmatrix}\mathbf{0} \\ \mathbf{z}_{j-1}^i\end{bmatrix} + \sum_{j=2}^{n} r_j\begin{bmatrix}\mathbf{0} \\ \mathbf{x}_j^i\end{bmatrix} \tag{22}$$

for all configurations $i = 1, \ldots, m$, where q_j and r_j are arbitrary constants.

Perhaps (22) never occurs, but for completeness we include its possibility. The new identifiability theorem can now be stated.

Theorem 3 (Fixed Endpoint Identifiability): For a redundant manipulator with fixed endpoint forming a closed kinematic chain that is not type-e, the parameters $\underline{\varphi}$ are locally unidentifiable, or locally nonunique, if and only if there exist constants c_j and k_j, not all zero, such that

$$0 = \sum_{j=1}^{n} c_j\mathbf{z}_{j-1}^i + \sum_{j=2}^{n} k_j\mathbf{x}_j^i \tag{23}$$

for all configurations $i = 1, \ldots, m$. Furthermore, the parameters of a type-e mechanism are nonunique, if (23) holds for the c_j and k_j restricted as above.

Proof: A modified Lemma 3 with (15) changed to (23) can be proven with the following alterations. Part 1 of the proof proceeds as before, with a final step using (21) to eliminate any $\mathbf{x}_1$ occurrences. This is always possible because the mechanism is not type-e. Part 2 proceeds as before. Lemma 4 holds if its proof is modified to use (15), with $\mathbf{x}_1^i$ eliminated, and (21) instead of (1). Alternatively, for all mechanism types, local nonuniqueness follows directly from (23) by adding (23) to (21) and remarking, as in the proof of Lemma 4, that the length parameters are nonunique. This theorem then follows. ■

For type-e mechanisms, the angle-dependent screw coordinates $(\mathbf{J}_\alpha^i)_j$ and $(\mathbf{J}_\theta^i)_j$ in (12) are linearly related by the length parameters as above. The orientation component of this linear screw relation gives (21) and the eliminations of $\mathbf{x}_1$ from (15) in Part 1 of the proof to Lemma 3 cannot proceed. We do not know if a type-e mechanism can actually occur and do not consider it further.

We now discuss two additional singularities in the closed-loop calibration procedure to the three singularities in the open-loop procedure that also apply here.

Singularity 4: Inherent Singularities in the Mechanism: Certain mechanisms have particular symmetries that allow the kinematics to be described in less than four parameters per joint. It is difficult to provide a general rule for when this will happen, but it is usually restricted to mechanisms of mobility one. A simple example is a 3-DOF planar manipulator that makes a point contact with the ground (Fig. 4). If the resulting closed-loop, four-bar linkage happens to be a parallelogram, then the opposite $\mathbf{x}$ axes are always parallel:

$$\mathbf{x}_2 + \mathbf{x}_4 = \mathbf{0}. \tag{24}$$

This satisfies the condition (23), and thus the lengths of the opposite sides, a_2 and a_4, are not identifiable (except as a sum). Clearly, this problem may be eliminated by having the manipulator change its endpoint location so that a parallelogram is not formed.

Singularity 5: Structural Immobility: If a particular joint j is immobile, then two consecutive joint coordinates are fixed relative to one another. This implies that $\mathbf{x}_j$, $\mathbf{z}_j$, $\mathbf{x}_{j-1}$, and $\mathbf{z}_{j-1}$ have a constant linear relation (satisfying (23)), as these four vectors span a three-dimensional space. Of course, it is not surprising that the parameters of the links connected by the immobile joint are unidentifiable. Conceivably a fictitious link that combined the two links could be defined and the rest of the mechanism identified.

To proceed, it is necessary to spot immobile joints. Following the approach in [24], we first determine whether the mechanism is totally immobile. Since the classical mobility definition [11] does not suffice for special mechanisms, the following condition is derived.

Lemma 5: A single-loop closed kinematic chain is mobile if and only if the columns of the Jacobian $\mathbf{J}_\theta^i$ are linearly dependent.

Proof: Let the screw coordinate $\$_j^i$ represent the jth column of $\mathbf{J}_\theta^i$. Since $\mathbf{J}_\theta^i \dot{\underline{\theta}}^i = \underline{0}$, then

$$\underline{0} = \dot{\theta}_1^i \$_1^i + \cdots + \dot{\theta}_n^i \$_n^i. \tag{25}$$

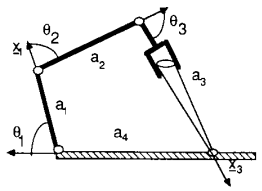

Fig. 4. A 3-DOF planar manipulator with a fixed point contact to ground.

All $\dot{\theta}_j^i$'s will be identically zero if and only if the joint screws $\$_j^i$ are independent. ■

Next we determine whether a single joint, say joint 1, is immobile. From (25), link one's instantaneous movement is $\dot{\theta}_1^i \$_1^i = -\dot{\theta}_n^i \$_n^i - \cdots - \dot{\theta}_2^i \$_2^i$. For link one to move, $\$_1^i$ must be a linear combination of the other screws. Stated otherwise, the space *span* $[\$_1^i]$ must intersect the space *span* $[\$_n^i, \ldots, \$_2^i]$ spanned by the other screws. The following result from linear algebra is useful [23].

Lemma 6: Let A and B be subspaces for a vector space V such that $V = A + B$ where $A + B = [v \mid v = a + b, a \in A, b \in B]$. Then

$$K(A \cap B) = K(A) + K(B) - K(V) \tag{26}$$

where $K(W)$ denotes the dimension of a vector space W.

For the following lemma, identify A with span $[\$_1^i]$ and B with span $[\$_n^i, \ldots, \$_2^i]$.

Lemma 7: Joint one will be mobile if and only if

$$1 + K\left(\text{span}\left[\$_n^i, \ldots, \$_2^i\right]\right) - K\left(\text{span}\left[\$_n^i, \ldots, \$_1^i\right]\right) > 0. \tag{27}$$

Any joint's mobility may be ascertained by (27) with the appropriate renumbering of the links.

As an example, consider the mechanism formed by rigidly fixing the hand of an anthropomorphic arm [13] relative to its shoulder (that is, imagine holding onto the desk in front of you). Although this mechanism has a classical mobility of 1 (7 minus 6), the elbow joint can be shown to be immobile. Consider the upper arm as the base link, so that $\$_1^i$ is the screw coordinate for the elbow (Fig. 5) Without loss of generality, one of the three wrist joint axes may be defined to intersect the shoulder joint. Thus the three shoulder joint axes and this wrist joint axis are linearly dependent, and $K(\text{span}[\$_2^i, \ldots, \$_7^i]) = 5$ whereas $K(\text{span}[\$_1^i, \ldots, \$_7^i]) = 6$. Therefore, (27) shows that the elbow joint is immobile. The solution to this problem is to relax the endpoint constraint so that the elbow is mobile; for example, only maintain a point contact with the ground, allowing arbitrary orientation of the hand. This solution requires a reformulation of the identification equations and is taken up in Section IV.

B. Simulations

This section presents two simulations, one for a 7-DOF manipulator and the other for two 6-DOF manipulators rigidly attached at their endpoints. In these and all subsequent examples the rank of the matrix $\mathscr{C}$ was monitored to avoid singularities. Furthermore, $\mathscr{C}$ has full rank for the actual parameters, and thus all mechanisms are identifiable.

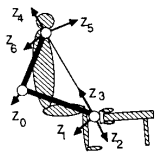

Fig. 5. Anthropomorphic arm screw coordinate assignment.

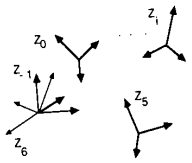

Fig. 6. Coordinate description of a manipulator under point contact.

Example 1: A 7-DOF manipulator, with actual D–H parameters in Table II, was formed into a closed-loop mechanism by the end effector grasping the ground at a fixed arbitrary position. This mechanism was simulated in 40 distinct configurations ($\theta_1 = 0$ to 0.5 rad). Starting with the initial guesses in Table I and with the definition $s_3 = 1$, the simulated joint angles were fed into the iterative Levenberg–Marquardt algorithm, and the parameters in Table II were recovered to within four decimal places.

Example 2: Two 6-DOF manipulators whose end-effectors are rigidly grasping together form the 12-DOF closed mechanism in Table IV. These parameters were used to simulate the movements of this mechanism into 40 different configurations ($\theta_j = 0$ to 0.5 rad, $j = 1$ to 6). With the initial parameters given in Table III and the simulated joint angles the calibration was performed (also $s_3 = 1$ fixed). The parameters in Table IV were recovered to within four decimal places.

TABLE I
7-DOF MECHANISM: INITIAL PARAMETERS

Joint	$\underline{s}$(m)	$\underline{a}$(m)	$\underline{\alpha}$(rad)	$\underline{\theta}^{off}$(rad)
1	1.694	0.837	3.774	1.100
2	1.622	−0.627	−0.553	0.080
3	1.000	−0.100	0.930	0.090
4	−0.430	−0.430	2.040	0.900
5	0.540	−0.600	−0.150	0.050
6	−0.560	−0.550	−1.350	0.040
7	−1.693	0.711	−1.859	0.000

TABLE II
7-DOF MECHANISM: CALIBRATED PARAMETERS

Joint	$\underline{s}$(m)	$\underline{a}$(m)	$\underline{\alpha}$(rad)	$\underline{\theta}^{off}$(rad)
1	1.594	0.737	3.604	0.000
2	1.722	−0.527	−0.503	0.000
3	1.000	0.000	0.530	0.000
4	−0.330	−0.330	2.300	0.000
5	0.440	−0.440	−0.900	0.000
6	−0.660	−0.550	1.200	0.000
7	−1.793	0.911	−1.459	1.825

TABLE III
12-DOF MECHANISM: INITIAL PARAMETERS

Joint	$\underline{s}$(m)	$\underline{a}$(m)	$\underline{\alpha}$(rad)	$\underline{\theta}^{off}$(rad)
1	−1.694	−0.837	3.504	0.100
2	−1.822	0.627	−0.553	0.050
3	1.000	0.100	0.580	0.070
4	0.430	0.430	2.380	1.070
5	−0.540	0.540	−0.980	0.080
6	0.760	0.650	1.280	0.050
7	1.200	0.760	−1.390	0.100
8	1.200	1.500	3.800	0.100
9	0.600	−1.400	1.550	0.200
10	0.300	1.100	−1.380	0.300
11	1.300	0.600	0.880	0.900
12	−1.982	−1.839	1.772	0.400

TABLE IV
12-DOF MECHANISM: CALIBRATED PARAMETERS

Joint	$\underline{s}$(m)	$\underline{a}$(m)	$\underline{\alpha}$(rad)	$\underline{\theta}^{off}$(rad)
1	−1.594	−0.737	3.604	0.000
2	−1.722	0.527	−0.503	0.000
3	1.000	0.000	0.530	0.000
4	0.330	0.330	2.300	0.000
5	−0.440	0.440	−0.900	0.000
6	0.660	0.550	1.200	0.000
7	1.100	0.660	−1.300	0.000
8	1.100	1.400	3.900	0.000
9	0.500	−1.300	1.400	0.000
10	0.200	1.000	−1.300	0.000
11	1.200	0.500	0.800	0.000
12	−1.882	−1.939	1.722	0.000

IV. Nonredundant Robot Calibration and Task Geometry Estimation

Next we extend the closed-loop method to situations where the end effector contact with the ground has some passive DOF's. Two examples, treated in detail shortly, are a manipulator opening a door (a 1-DOF task) and a manipulator under point contact (a 3-DOF task). If t is the number of task DOF's, then the mobility of the resultant closed chain is $n + t - 6$. For the door-opening task, 6-DOF nonredundant manipulators can therefore be calibrated. For the point contact task, manipulators with as few as 4 DOF's may be calibrated. At the same time, the geometry of the task is calibrated.

Since the passive task DOF's are unsensed, they must be eliminated from the 6 kinematic loop closure equations. Up to five unsensed DOF's may be eliminated to leave at least one equation for the identification procedure. This elimination is simple for the door-opening and point-contact tasks but more difficult for arbitrary task kinematics.

A. Point Contact

An n-DOF manipulator under point contact is equivalent to grasping a passive spherical ball joint. There are three passive DOF's at the endpoint corresponding to orientation that are unsensed. Hence the orientation equations in the previous calibration procedure cannot be used, but the three position equations (20) can. Again, define the base origin to coincide with the endpoint position. For example, for the 6-DOF manipulator in Fig. 6, the position of the base coordinates (subscript -1) is coincident with that of the endpoint coordinates (subscript 6). The orientation of the -1

coordinates is arbitrary with respect to the 0 coordinates, so θ_0^{off} and α_0 are taken as arbitrary constants. Moreover, the orientation of the end effector coordinates is arbitrary with respect to the five coordinates; hence α_6 (or more generally α_n) is taken as an arbitrary constant also. Finally, it is necessary to specify one length parameter; for the theorem below, we select $a_0 = -1$.

To incorporate just the position equations, we redefine $\underline{x}_c^i = \mathbf{p}_c^i = \mathbf{0}$ from (3) and $\Delta\underline{x}_c^i = (dx_c^i, dy_c^i, dz_c^i)$ from (7). The constant parameters θ_0^{off}, α_0, α_n, and a_0 are removed from φ. Then $\mathscr{X}$, $\mathscr{F}$, $\mathscr{C}$, and $\mathbf{C}^i$ are redefined in (4)–(5) and (8) to reflect the reduced dimensions. In particular, each column of each Jacobian in (12) contains only the bottom three rows.

$$(\mathbf{J}_a^i)_j = \mathbf{x}_j^i, (\mathbf{J}_s^i)_j = \mathbf{z}_{j-1}^i, (\mathbf{J}_{\theta j}^o) = \mathbf{z}_{j-1}^i \times \mathbf{b}_j^i,$$
$$(\mathbf{J}_\alpha^i)_j = \mathbf{x}_j^i \times \mathbf{b}_{j+1}^i \quad (28)$$

These columns are now interpreted as *partial velocity* vectors with respect to the parameters instead of as screw coordinates [8]. Notice that we have used up three kinematic equations in order to eliminate the unmeasured orientation DOF's of the endpoint. The identification procedure can then be applied as before.

As before, the identifiability of the parameters depends on the linear dependence of the columns of the Jacobian $\mathbf{C}^i$. Because of the form of the columns in (28), a stronger identifiability condition than (16) is derived.

Theorem 4 (Point-Contact Identifiability): The parameters φ are unidentifiable if and only if there is a constant linear relation among the partial velocity vectors for all configurations. That is, there exist constants c_j^k, $k = 1, \ldots, 4$, not all zero, such that

$$\mathbf{0} = \sum_{j=0}^{n} c_j^1 \mathbf{z}_{j-1}^i + \sum_{j=1}^{n} c_j^2 \mathbf{z}_{j-1}^i \times \mathbf{b}_j^i + c_j^3 \mathbf{x}_j^i + \sum_{j=1}^{n-1} c_j^4 \mathbf{x}_j^i \times \mathbf{b}_{j+1}^i \quad (29)$$

for all $i = 1, \ldots, m$.

Again, trivial modifications to the theorem can be made if a different length parameter than a_0 is fixed.

We now simulate a 6-DOF manipulator under point contact; the actual parameters are given in Table VI. The arbitrary constant parameters are marked with an asterisk, and in particular we have chosen $s_2 = 1$ as the fixed-length parameter. This entire mechanism was simulated in 30 distinct configurations ($\theta_1, \theta_2, \theta_3 = 0$ to 0.5 rad), starting with the initial guesses in Table V. The parameters in Table VI were recovered to within four decimal places.

B. Opening a Door

The hinge joints of a door define a rotary axis. Since the endpoint coordinates are arbitrary, it is convenient to make $\mathbf{z}_n^i$ coincident with the door's axis (Fig. 7). We also position the base coordinates at the endpoint coordinates, and let $\mathbf{z}_{-1}^i$ coincide with $\mathbf{z}_n^i$. The door hinge angle θ_z^i measured about $\mathbf{z}_{-1}^i$ is unknown, and the orientation equation relating to this rotation must be eliminated from the calibration procedure.

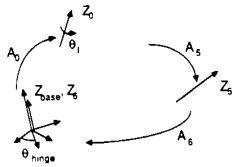

Fig. 7. The coordinate description of a manipulator connected to a hinge joint.

TABLE V
THE INITIAL D-H PARAMETERS OF A 6-DOF MANIPULATOR UNDER POINT CONTACT

Joint	$\underline{s}$(m)	$\underline{a}$(m)	$\underline{\alpha}$(rad)	$\underline{\theta}^{\text{off}}$(rad)
0	1.694	0.837	3.600*	0.000*
1	1.622	−0.627	−0.553	0.100
2	1.000*	−0.100	0.930	0.090
3	−0.430	−0.430	2.040	0.100
4	0.540	−0.600	−0.150	0.050
5	−0.560	−0.550	1.350	0.040
6	−1.693	0.711	−1.860*	1.700

TABLE VI
THE ACTUAL/CALIBRATED D-H PARAMETERS OF A 6-DOF MANIPULATOR UNDER POINT CONTACT

Joint	$\underline{s}$(m)	$\underline{a}$(m)	$\underline{\alpha}$(rad)	$\underline{\theta}^{\text{off}}$(rad)
0	1.594	0.737	3.600*	0.000*
1	1.722	−0.527	−0.503	0.120
2	1.000*	0.000	0.530	0.000
3	−0.330	−0.330	2.300	0.000
4	0.440	−0.440	−0.900	0.000
5	−0.660	−0.550	1.200	0.000
6	−1.793	0.911	−1.860*	1.825

To begin, the position equations are the same as before: $\mathbf{p}_c^i = \mathbf{0}$ from (3) and $\Delta\mathbf{p}^i = (dx_c^i, dy_c^i, dz_c^i)$ from (7). The endpoint orientation is given by

$$\mathbf{R}_c^i = \mathbf{R}_x(\partial x_c^i)\mathbf{R}_y(\partial y_c^i)\mathbf{R}_z(\theta_z^i) \quad (30)$$

where ∂x_c^i and ∂y_c^i are infinitesimal and θ_z^i is finite. Expanding the first column of (30) and neglecting the second-order terms, one finds that $\theta_z^i = \text{a tan}2(\mathbf{R}_{c(2,1)}^i, \mathbf{R}_{c(1,1)}^i)$, where the indices denote the elements of the rotation matrix $\mathbf{R}_c^i$. The desired variations ∂x_c^i and ∂y_c^i are extracted from $\mathbf{R}_c^i\mathbf{R}_z(\theta_z^i)^T = \mathbf{R}_x(\partial x_c^i)\mathbf{R}_y(\partial y_c^i)$. The computed endpoint location is then given by the five-vector $\underline{x}_c^i = (dx_c^i, dy_c^i, dz_c^i, \partial x_c^i, \partial y_c^i)$. Thus one kinematic equation has been used up in order to eliminate the unmeasured door hinge angle.

As before, one length parameter needs to be specified, say $a_1 = -1$. Since $\mathbf{z}_{-1}^i$ aligns with the door hinge and with $\mathbf{z}_n^i$, then θ_0^{off} and θ_0 can be arbitrarily set to zero. φ is adjusted to eliminate a_1 and θ_0^{off}. Finally, $\mathscr{X}$, $\mathscr{F}$, $\mathscr{C}$, and $\mathbf{C}^i$ are redefined in (4), (5), and (8) to reflect the reduced dimensions of $\underline{x}_c^i$. The kinematic calibration procedure may then be applied. Once again, identifiability is related to the rank of $\mathbf{C}^i$.

Next we simulate a 6-DOF manipulator grasping a door with a hinge joint. The D-H parameters are given in Table VIII; arbitrary parameters are marked by an asterisk, including the fixed length $s_3 = 1$. This entire mechanism was

simulated in 40 distinct configurations ($\theta_1 = 0$ to 0.5 rad), starting with the initial guesses in Table VII. The parameters in Table VIII were recovered to within four decimal places.

C. Identifying Arbitrary Task Kinematics

We now discuss how the algorithm presented for closed-loop kinematic calibration readily generalizes to identifying arbitrary task kinematics. As mentioned earlier, the chief difficulty is eliminating the unknown DOF's, from the environment kinematics. This may be achieved by determining the unknown DOF's in terms of the known ones (and the kinematic parameters). For instance, in calibrating a system comprised of a robot opening a door with a handle, both the door hinge angle and the handle angle may be determined in terms of the known manipulator joint angles. Once all of the DOF's are determined, the iterative identification algorithm presented above is directly applicable to identifying the kinematic parameters. In particular, the overdetermined system of equations (8) may be solved by the iterative Levenberg–Marquardt algorithm.

Determining the unknown DOF's may proceed as follows: 1) using the nominal model of the robot, compute the location of the endpoint at a specific configuration, then 2) notice that this endpoint also locates the endpoint of the environment kinematic chain, and finally 3) using the nominal kinematics of the environment calculate the inverse kinematic solution of the endpoint position given in step 1). The resulting joint angles are the unknown DOF's. The inverse kinematics of step 3) must in, general, be performed iteratively (e.g., with [18]). Notice that a nominal model of the kinematics is required. Each iteration of kinematic calibration algorithm presented in Section 3 improves the nominal model. Thus, the above determination of joint angles must be performed anew for each step of the kinematic calibration iteration.

V. Discussion

We have presented a new kinematic calibration method that does not require endpoint measurements or precision points. By forming manipulators into mobile closed kinematic chains, we have shown that consistency conditions in the kinematic loop closure equations are adequate to calibrate the manipulator from joint angle readings alone. This closed-loop kinematic calibration method is an adaptation of an iterative least-squares algorithm used in calibrating open-chain manipulators.

Identifiability of the kinematic parameters of the closed loop was reduced to inspecting the rank of the Jacobian matrix $\mathscr{C}$. Rank degeneracies were then studied with the screw coordinate interpretation of the columns of the Jacobians $\mathbf{C}^i$. Specifically, a requirement that there be no constant linear relation among the local link $\mathbf{x}_j^i$ and $\mathbf{z}_j^i$ axes accounts for all singularities when there are no passive DOF's. Closed mechanisms with passive DOF's must be studied on a case by case basis for identifiability.

Three tasks were studied in detail: 1) fixed endpoint, 2) point contact, and 3) opening a door. Nevertheless, the method readily generalizes to a large class of robot tasks.

TABLE VII
The Initial D-H Parameters for a 6-DOF Manipulator Opening a Door

Joint	$\underline{s}$(m)	$\underline{a}$(m)	$\underline{\alpha}$(rad)	$\underline{\theta}^{\text{off}}$(rad)
0	1.694	0.837	3.744	*
1	1.622	−0.627	−0.553	0.080
2	1.000	−0.100	0.930	0.090
3	−0.430	−0.430	2.040	0.900
4	0.540	−0.600	−0.150	0.050
5	−0.560	−0.550	1.350	0.040
6	−1.693	0.711	−1.859	1.400

TABLE VIII
The Actual/Calibrated D-H Parameters of a 6-DOF Manipulator Opening a Door

Joint	$\underline{s}$(m)	$\underline{a}$(m)	$\underline{\alpha}$(rad)	$\underline{\theta}^{\text{off}}$(rad)
0	1.594	0.737	3.604	*
1	1.722	−0.527	−0.503	0.000
2	1.000	0.000	0.530	0.000
3	−0.330	−0.330	2.300	0.000
4	0.440	−0.440	−0.900	0.000
5	−0.660	−0.550	1.200	0.000
6	−1.793	0.911	−1.459	1.825

The main requirement is that there be positive mobility in the closed chain; in general, the sum of manipulator DOF's plus the passive DOF's of the endpoint constraint must exceed six. Fixed endpoint constraints generally require redundant arms to achieve positive mobility. An equivalent scenario is two manipulators rigidly attached at their endpoints with combined DOF's greater than six; thus two nonredundant arms could be calibrated together. When passive endpoint constraints are allowed, single nonredundant arms may be calibrated as well; for example, under point contact the manipulator only requires 4 DOF's. In principle, up to five passive DOF's can be allowed in the endpoint. For every passive DOF, one of the six kinematic loop closure equations is used up to eliminate the unknown joint angle; this procedure is akin to mechanism synthesis.

In our method, it is necessary to specify one length parameter to scale the mechanism. An independent means for measuring this parameter is required. This is a feature of other kinematic calibration methods as well, such as those using theodolites [27].

Another issue with our method is how to handle the forces encountered when moving the manipulator with an inaccurate kinematic model under endpoint constraints. It is beyond the scope of this paper to present a detailed solution, but an appropriate force control procedure must be implemented. The task is made easier if the joint actuation is inherently complaint. For example, one could drive only as many joints as there are degrees of mobility in the loop. Alternatively, one could drive all joints using the initial guess at the kinematic parameters to calculate the constrained joint motion, and then rely on the joint compliance to allow for error in the commanded joint trajectories. Although more complicated, this latter method is better, as the former method could lead to the drive joints jamming at singularities. Recently, we applied our method to calibrating two fingers of the Utah/MIT Dextrous Hand, which were rigidly attached at the endpoints

to form a closed-loop mechanism with 8 DOF's [6]; the fingers were moved manually as a simple remedy in this particular case.

Although the joint offsets $\underline{\theta}^{\text{off}}$ were the only nongeometric parameters modeled in this paper, in principle more complicated nongeometric joint models could be calibrated. For example, in [6] an additional scaling factor for the joint angle sensors was required and successfully identified.

Our closed-loop method to kinematic calibration represents a departure from the typical dichotomy found in robotics between model building and task performance. The removal of this dichotomy may generalize to other problem areas in robotics. In this paper, the models of the task and the manipulator are improved *while* the task is being performed. In a separate paper, we have also shown how an uncalibrated stereo vision system can be calibrated together with an uncalibrated manipulator [7]. Thus we feel that our approach is a step toward true autonomy: no special precalibrated endpoint measurement device—or external "teacher"—is needed.

References

[1] C. H. An, C. G. Atkeson, and J. M. Hollerbach, *Model-based Control of a Robot Manipulator.* Cambridge, MA: MIT Press, 1988.

[2] B. Armstrong, "On finding 'exciting' trajectories for identification involving systems with non-linear dynamics," in *Proc. IEEE Int. Conf. Robotics Automat.* (Raleigh, NC, Mar. 31-Apr. 3, 1987) pp. 1331-1139.

[3] D. J. Bennett and J. M. Hollerbach, "Self-calibration of single-loop, closed kinemattic chains formed by dual or redundant manipulators," in *Proc. 27th IEEE Conf. Decision Contr.* (Austin, TX, Dec. 7-9, 1988) pp. 627-629.

[4] ——, "Identifying the kinematics of robots and their tasks," in *Proc. IEEE Int. Conf. Robotics Automat.* Scottsdale, AZ, May 14-19, 1989) pp. 580-586.

[5] ——, "Identifying the kinematics of non-redundant serial chain manipulators by a closed-loop approach," in *Proc. 4th Int. Conf. Advanced Robotics* (Columbus, OH, June 13-15, 1989), pp. 514-524.

[6] ——, "Closed-loop kinematic calibration of the Utah-MIT Hand," in *Experimental Robotics I – The First International Symposium*,V. Hayward and O. Khatib, Eds. New York: Springer-Verlag, 1990, pp. 539-552.

[7] D. J. Bennett, J. M. Hollerbach, and D. Geiger, "Autonomous robot calibration for hand-eye coordination," in *Preprints 5th Int. Symp. Robotics Res.* (Tokyo, Aug. 28-31, 1989), pp. 148-155.

[8] J. W. Burdick, "Kinematics analysis and design of redundant manipulators," Ph.D. dissertation, Stanford University, Palo Alto, CA, Mar. 1988.

[9] J. Denavit and R. S. Hartenberg, "A kinematic notation for lower pair mechanisms based on matrices," *J. Appl. Mech.*, vol. 22, pp. 215-221, 1955.

[10] V. Guilleman and A. Pollack, *Differential Topology.* Englewood Cliffs, NJ: Prentice-Hall, 1974.

[11] R. S. Hartenberg and J. Denavit, *Kinematic Synthesis of Linkages.* New York: McGraw-Hill, 1964.

[12] S. A. Hayati, "Robot arm geometric link parameter estimation," in *Proc. 22nd IEEE Conf. Decision Cont.* (San Antonio, TX, Dec. 14-16, 1983), pp. 1477-1483.

[13] J. M. Hollerbach, "Optimum kinematic design for a seven degree of freedom manipulator," *Robotics Research: The Second International Symposium,* eds. H. Hanafusa and H. Inoue. Cambridge, MA: MIT Press, 1985, pp. 349-356.

[14] ——, "A review of kinematic calibration," in *The Robotics Review I,* O. Khatib, J. J. Craig, and T. Lozano-Perez, Eds. Cambridge, MA: MIT Press, 1989, pp. 207-242.

[15] J. M. Hollerbach and D. J. Bennett, "Automatic kinematic calibration using a motion tracking system," *Robotics Research: the Fourth International Symposium,* R. Bolles and B. Roth, Eds. Cambridge, MA: MIT Press 1988; pp. 191-198.

[16] H. Lee and C. Liang, "Displacement analysis of the general spatial 7-link 7R Mechanism," *Mech. Mach. Theory,* vol. 23, pp. 219-226, 1988.

[17] B. W. Mooring, Z. S. Roth, and M. R. Driels, *Fundamentals of Manipulator Calibration.* New York: Wiley-Interscience, 1991.

[18] Y. Nakamura and H. Hanafusa, "Inverse kinematic solutions with singularity robustness for robot manipulator control," *J. Dynamic Syst., Meas., Contr.,* vol. 108, pp. 163-171, 1986.

[19] J. P. Norton, *An Introduction to Identification.* Orlando, FL: Academic, 1986.

[20] B. Roth, "Screws, motors, and wrenches that cannot be bought in a hardware store," in *Robotics Research: The First International Symposium,* M. Brady and R. Paul, Eds. Cambridge, MA: MIT Press, 1984, pp. 679-693.

[21] N. K. Sinha and B. Kuszta, *Modeling and Identification of Dynamic Systems.* New York: Van Nostrand Reinhold, 1983.

[22] M. Spivak, *Calculus on Manifolds.* New York: W. A. Benjamin, 1965.

[23] G. Strang, *Linear Algebra and Its Applications.* New York: Academic, 1980.

[24] K. Sugimoto and T. Okada, "Compensation of positioning errors caused by geometric deviations in robot system," in *Robotics Research: The Second International Symposium,* H. Hanafusa and H. Inoue, Eds. Cambridge, MA: MIT Press, 1985, pp. 231-236.

[25] C. W. Wampler II, "Manipulator inverse kinematic solutions based on vector formulations and damped least-square methods," *IEEE Trans. Syst. Man, Cybern.,* vol. SMC-16, pp. 93-101, 1986.

[26] D. E. Whitney, "The mathematics of coordinate control of prosthetic arms and manipulators," *J. Dynamic Syst., Meas., Cont.,* pp. 303-309, 1972.

[27] D. E. Whitney, C. A. Lozinski, and J. M. Rourke, "Industrial robot forward calibration method and results," *J. Dynamic Syst. Meas., Control,* vol. 108, pp. 1-8, 1986.

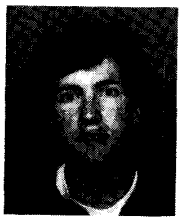

David J. Bennett (S'91) received the B.Eng. degree in electrical engineering in 1984 from McGill University, Montreal, and the Ph.D. degree in brain and cognitive sciences in 1990 from the Massachusetts Institute of Technology, Cambridge.

He is currently a Post-Doctoral Associate at the MIT Department of Brain and Cognitive Sciences. His interests include system identification, motor control, and robotics.

John M. Hollerbach (M'85) received the B.S. degree in chemistry and the M.S. degree in mathematics from the University of Michigan, Ann Arbor, in 1968 and 1969, respectively, and the Ph.D. degree in computer science from the Massachusetts Institute of Technology, Cambridge, in 1978.

He is currently the Natural Sciences and Engineering/Canadian Institute for Advanced Research Professor of Robotics at McGill University, Montreal, jointly in the Departments of Mechanical Engineering and Biomedical Engineering. He has published several books and many papers in the area of robotics and biological motor control.

Dr. Hollerbach received an NSF Presidential Young Investigator Award in 1984. He was Co-Chairman of the 1985 Engineering Foundation Conference on Biomechanics and Neural Control of Movement and the Program Chairman of the 1989 IEEE International Conference on Robotics and Automation. He serves as a Technical Editor of the IEEE TRANSACTIONS ON ROBOTICS AND AUTOMATION and as a member of the Administrative Committee of the IEEE Robotics and Automation Society.